LOSS OF THE TUMOR SUPPRESSOR, TP53, ENHANCES THE ANDROGEN RECEPTOR MEDIATED ONCOGENIC TRANSFORMATION AND TUMOR DEVELOPMENT IN THE MOUSE PROSTATE

Yongfeng He[1,4,¶], **Daniel T. Johnson**[1,¶], **Julie S. Yang**[1,¶], **Huiqing Wu**[2,¶], **Sungyong You**[6,¶], **Junhee Yoon**[6], **Dong-Hong Lee**[1], **Won Kyung Kim**[1], **Joseph Aldahl**[1], **Vien Le**[1], **Erika Hooker**[1,4], **Eun-Jeong Yu**[1,4], **Joseph Geardts**[3], **Robert D. Cardiff**[5], **Zijie Sun**[1,4,*]

[1]Department of Cancer Biology, Beckman Research Institute, City of Hope, Duarte, CA 91010-3000

[2]Department of Pathology, Beckman Research Institute, City of Hope, Duarte, CA 91010-3000

[3]Department of Population Sciences, Beckman Research Institute, City of Hope, Duarte, CA 91010-3000

[4]Department of Urology, Stanford University School of Medicine, Stanford, CA 94305-5328

[5]Center for Comparative Medicine, University of California at Davis, 4115 Primate Research Drive, Davis CA 95616

[6]Division of Cancer Biology and Therapeutics, Departments of Surgery, Samuel Oschin Comprehensive Cancer Institute, Cedars-Sinai Medical Center, Los Angeles, CA, 90048.

Abstract

Recent genome analysis of human prostate cancers demonstrated that both *AR* gene amplification and *TP53* mutation are among the most frequently observed alterations in advanced prostate cancer. However, the biological role of these dual genetic alterations in prostate tumorigenesis is largely unknown. In addition, there are no biologically relevant models that can be used to assess the molecular mechanisms for these genetic abnormalities. Here, we report a novel mouse model, in which elevated transgenic *AR* expression and *Trp53* deletion occur simultaneously in mouse prostatic epithelium to mimic human prostate cancer cells. These compound mice developed an earlier onset of high-grade prostatic intraepithelial neoplasia and accelerated prostate tumors in comparison to mice harboring only the AR transgene. Histological analysis showed prostatic sarcomatoid and basaloid carcinomas with massive squamous differentiation in the above compound mice. RNA-sequencing analyses identified a robust enrichment of the signature genes for human prostatic basal cell carcinomas in the above prostate tumors. Master Regulator Analysis

*To whom correspondence should be addressed: Zijie Sun, Ph.D, MD, Department of Cancer Biology, Beckman Bldg., Room 2311, 1500 E. Duarte Rd., Duarte, CA 91010-3000: Tel: 626-218-0955; zjsun@coh.org.
¶These five authors contribute to the work equally

The authors declare no potential conflicts of interest

revealed SOX2 as a transcriptional regulator in prostatic basal cell tumors. Elevated expression of SOX2 and its downstream target genes were detected in prostatic tumors of the compound mice. Chromatin immunoprecipitation analyses implicate a co-regulatory role of AR and SOX2 in the expression of prostatic basal cell signature genes. Our data demonstrate a critical role of SOX2 in prostate tumorigenesis and provide mechanistic insight into prostate tumor aggressiveness and progression mediated by aberrant AR and p53 signaling pathways.

Keywords

Prostate Cancer; The androgen receptor; p53 tumor suppressor; knockout mice; SOX2

INTRODUCTION

Emerging evidence has shown an essential role of androgen signaling in prostate tumorigenesis [1]. Thus, androgen deprivation therapy (ADT) inhibiting androgen signaling-mediated cell growth and survival has been widely used to treat prostate cancer [2]. Conditional expression of the *AR* transgene in the mouse prostate induces both prostatic intraepithelial neoplasia (PIN) and prostatic carcinoma development in aged mice [3], which provides direct evidence for the oncogenic role of the AR in prostate tumorigenesis. The AR is consistently expressed in a majority of prostate cancer samples before and after the therapy [4–6]. In fact, *AR* gene amplification appears in one-third of prostate cancer samples even after androgen deprivation therapy [7, 8]. Recent integrative cancer genomic analyses have further demonstrated that the alteration of androgen signaling is a key cellular event during prostate cancer initiation, progression, and metastasis [9, 10].

The tumor suppressor p53 is a sequence-specific DNA-binding transcription factor that regulates the cell cycle checkpoint pathway in response to DNA damage [11]. Although the *TP53* gene is the most frequent target for genetic alterations in cancer [6, 12], its role in prostate tumorigenesis remains unclear. Li-Fraumeni patients carrying germline *TP53* mutations have a low incidence of prostate cancer in comparison to other human malignancies [13]. Either heterozygous or homozygous deletion of *Trp53* in mouse prostatic epithelium fails to induce oncogenic transformation [14, 15]. Genetic alteration of the *TP53* appears less in early invasive carcinoma than in advanced, recurrent, and metastatic prostate cancer [16]. Specifically, it has become the second most common alteration in castration resistant prostate cancer, CRPC [6, 17].

Recent genomic studies have shown that the co-occurrence of *AR* gene amplification and *TP53* deletion is one of the most frequent abnormal alterations in CRPC [6, 8]. To explore the collaborative role of dysregulation of both AR and p53 in prostate tumorigenesis, we generated a mouse model in which elevated transgenic *AR* expression and *Trp53* deletion occur simultaneously in mouse prostatic epithelium to mimic what happens in human prostate cancer cells. The compound mice developed an earlier onset of high-grade PIN and an accelerated prostate tumor lesions in comparison with the *AR* transgenic mice [3]. Intriguingly, pathological changes resembling prostatic sarcomatoid and basaloid carcinomas with massive squamous differentiation were revealed in the compound mice.

RNA-sequencing analyses showed a robust enrichment of the signature genes for human prostatic basal cell carcinomas in prostate tumor samples from the compound mice [18]. Master Regulator Analysis (MRA) identified SOX2, SUZ12, and MTF2 as top candidates for master transcriptional regulators in the above prostatic tumor samples. Elevated expression of SOX2 and its downstream target genes were detected in the prostatic tumor samples of the compound mice. Chromatin immunoprecipitation analyses (ChIP) revealed an increase in recruitment of SOX2 and AR on the regulatory loci of their target genes in the compound mouse tumor tissues. In addition, increased co-occupancies of AR and SOX2 on the regulatory loci of their target genes were also revealed in the above tumor cells. These results demonstrate a regulatory role of SOX2 in prostate tumorigenesis and elucidate a novel mechanism underlying elevated *AR* expression and *Trp53* deletion-induced prostate cancer progression, aggressiveness, and trans-differentiation.

RESULTS

Generating the conditional AR transgenic and Trp53 deletion mice

Genetic analyses of prostate cancer clinical cohorts showed a significant co-occurrence of alterations of the *AR* and *TP53* genes (Log odds ratio=1.257, p-value<0.001) [19]. *AR* amplification was detected in 459 prostate cancer samples, among which 44% of the samples also are altered for the *TP53* gene (Fig. 1A). The majority of patients (87%) bearing both amplified *AR* and *TP53* alteration were diagnosed with metastatic CRPC (Fig. 1B), providing a direct association between these dual genetic alterations and the pathogenesis of advanced prostate cancer. Given the significance and prevalence of the AR and p53 abnormalities in human prostate cancers, we generated $p53^{L/+}/R26^{hAR/+}$:Osr1-Cre and $p53^{L/L}/R26^{hAR/+}$:Osr1-Cre compound mice to directly assess the biological role of *AR* and *Trp53* aberrations in prostate tumorigenesis (Fig. 1C). In these compound mice, loss of or reduced *Trp53* expression and elevated *AR* expression simultaneously occur in prostatic epithelium through *Osr-1* promoter-driven *Cre* expression [3, 20]. The activity of *Osr1-Cre* was assessed for the *AR* transgene and *Trp53* floxed alleles in different mouse tissues using genomic PCR approaches. A 300 bp (blue empty arrow) or 500 bp (red empty arrow) PCR fragment, corresponding to the deletion of either the LSL cassette on the *AR* transgene alleles or exon 2–10 of *Trp53* deleted alleles, respectively, were observed in mouse prostate, bladder, and lung tissues (Fig. 1D). IHC analyses further confirmed the loss of p53 with or without expression of transgenic AR protein in prostate tissues of $p53^{L/L}$:Osr1-Cre, $R26^{hAR/+}$:Osr1-Cre, and $p53^{L/L}/R26^{hAR/+}$:Osr1-Cre mice, respectively (Fig. 1E–J). These above results demonstrate the expression of the *AR* transgene and deletion of *Trp53* in the prostate of the compound mice.

Conditional deletion of Trp53 in the mouse prostate enhances transgenic AR mediated oncogenic transformation

All mice, including $p53^{L/L}$:Osr1-Cre, $p53^{L/+}$:Osr1-Cre, $R26^{hAR/+}$:Osr1-Cre, $p53^{L/+}/R26^{hAR/+}$:Osr1-Cre, and $p53^{L/L}/R26^{hAR/+}$:Osr1-Cre mice, were born at the expected Mendelian ratios and appeared normal with no obvious differences from their wild-type littermates at birth. Prostate tissues were isolated from the above male mice at 2, 3, 4, 6, 9, 12, and 18 months of age and analyzed adhering to recommendations of the Mouse Models

of Human Cancers Consortium Prostate Pathology Committee [21]. Examination of prostate tissues from 2–18 month old *p53^{L/L}:Osr1-Cre* and *p53^{L/+}:Osr1-Cre* mice showed normal glands in all prostate lobes, including the anterior (AP), dorsal (DP), lateral (LP), and ventral (VP) lobes (Fig. 2A–B', and 2I, and Supplemental Fig. 1A and 1B). Our observations were consistent with previous studies [14, 22] and suggest that the deletion of *Trp53* in the mouse prostate was insufficient to initiate oncogenic transformation. The *AR* transgenic mice, *R26^{hAR/+}:Osr1-Cre*, developed low-grade prostatic intraepithelial neoplasia (LGPIN) at the age of three months (Fig 2C–C', and supplemental Fig. 1C1–1C1'). Strikingly, the compound mice bearing both *Trp53* deletion and transgenic *AR* expression showed more aggressive PIN lesions at age of three months (Fig. 2D–E', 2I, and Supplemental Fig. 1D1–E3). These results demonstrate that *Trp53* deletion synergistically enhances AR-mediated oncogenic transformation in the mouse prostate.

IHC analyses were carried out to assess the cellular properties of PIN lesions using a series of adjacent tissue sections isolated from three-month-old mice of different genotypes. Uniform nuclear staining with the human AR antibody was observed in most atypical prostatic cells within PIN lesions in *R26^{hAR/+}:Osr1-Cre* mice, *p53^{L/+}/R26^{hAR/+}:Osr1-Cre* and *p53^{L/L}/ R26^{hAR/+}:Osr1-Cre* compound mice, providing a direct link between transgenic *AR* expression and PIN formation (Fig. 2F1, 2G1, and 2H1). The robust staining of both E-cadherin (Fig. 2F2) and CK8 (Fig. 2F3) secretory and luminal epithelial cell markers, was revealed in the atypical cells in the PIN lesions of *R26^{hAR/+}:Osr1-Cre* mice. In contrast, only reduced staining of E-cadherin and CK8 appeared in the PIN lesions of *p53^{L/+}/ R26^{hAR/+}:Osr1-Cre* and *p53^{L/L}/R26^{hAR/+}:Osr1-Cre* compound mice (Fig. 2G2–3 and 2H2–3). Interestingly, the staining of CK5, a basal epithelial cell marker, was exclusively within the basal compartment of PIN lesions of *R26^{hAR/+}:Osr1-Cre* mice (Fig. 2F4), while extensive staining was throughout the PIN regions of the compound mice (Fig. 2G4 and 2H4). Expression of p63 was revealed within the periphery of the basal layer (Fig. 2F5, 2G5, and 2H5) and no staining for synaptophysin (Fig. 2F6, 2G6, and 2H6) was observed in PIN lesions of *AR* transgenic or compound mice. The above data demonstrate the basal cell properties of the PIN lesions in both *p53^{L/+}/R26^{hAR/+}:Osr1-Cre* and *p53^{L/L}/ R26hAR^{/+}:Osr1-Cre* compound mice, suggesting a regulatory role of *Trp53* deletion in inducing atypical cell trans-differentiation.

Conditional expression of the AR transgene and deletion of Trp53 accelerate tumor formation in the mouse prostate

Following the consensus that high-grade mPIN lesions can progress to prostate adenocarcinomas, we continued examining different genotypes of mice for extended periods of time. Strikingly, both *p53^{L/+}/R26^{hAR/+}:Osr1-Cre* and *p53^{L/L}/R26^{hAR/+}:Osr1-Cre* compound mice developed visible prostatic tumors starting at 6-months of age, which is earlier than *R26^{hAR/+}:Osr1-Cre* mice (Fig. 2I). Typical prostatic adenocarcinoma lesions were observed in *R26^{hAR/+}:Osr1-Cre* mice as reported previously [3] (Supplemental Fig. 2A–A2 and B–B2). However, prostate tumor tissues from the compound mice revealed pathological lesions reflecting a diversity of aggressive tumor phenotypes (Fig. 3A–C). These included adenosquamous carcinoma comprised of glandular structures and keratinizing cells with intercellular bridges (Fig. 3A1–1'), basaloid carcinoma comprised of

relatively small cells with scant cytoplasm and a high nuclear/cytoplasmic ratio (Fig. 3A2–2'), and sarcomatoid areas comprised of markedly atypical spindle cells in $p53^{L/+}/R26^{hAR/+}$:Osr1-Cre tumor tissues (Fig. 3A3–3'). Similar pathological features were also revealed in prostatic tumors of $p53^{L/L}/R26^{hAR/+}$:Osr1-Cre mice (Fig. 3B), including invasive tumors with squamous (Fig. 3B1–1'), basaloid (Fig. 3B2–2') and sarcomatoid (Fig. 3B3–3') trans-differentiation. The squamous areas were remarkable for prominent extracellular keratin with formation of numerous "pearls", but glandular structures were not apparent. To assess the cellular properties of the prostatic tumor lesions above, we performed IHC analyses and confirmed the luminal cell properties of prostatic tumors in $R26^{hAR/+}$:Osr1-Cre mice (Supplemental Fig. 3A1–G1), which was consistent with previous reports [3]. The majority of tumor cells in prostate tissues of $p53^{L/+}/R26^{hAR/+}$:Osr1-Cre and $p53^{L/L}/R26^{hAR/+}$:Osr1-Cre compound mice showed positive staining for AR and E-cadherin (Supplemental Fig. 3B2–3 and 3C2–3). However, these cells also revealed weak staining for CK8 but strong staining for CK5 and p63 (Supplemental Fig. 3), suggesting their basal cell properties. Using a series of adjacent sections of the compound mouse tumor tissues, we further demonstrated the basal cell property of tumor cells in the above lesions, featuring positive staining for CK5, E-cadherin, and human AR but negative for CK8 (Fig. 4A–E). In addition, squamous tumor lesions were also identified in the tumor tissues. As shown in Fig, 4F–J, tumor cells showed positive staining to CK5, 6, and 10 [23], but very few cells were positive for CK8. Positive staining for transgenic human AR appeared in both basaloid and squamous tumor cells (Fig. 4K), implying their origins from the transgenic *AR*-expressing cells. The above results demonstrate that loss of p53 synergistically enhances AR-mediated prostate tumor formation and induces tumor cell trans-differentiation to promote aggressive tumor phenotypes.

Enrichment of cell signaling pathways related to aggressive tumor phenotypes and disease progression in prostate tumors of AR transgenic and Trp53 deletion compound mice

In search of the molecular basis for the collaborative role of transgenic *AR* expression and *Trp53* deletion in prostate tumorigenesis, we performed RNA-sequencing (RNA-seq) to examine the global transcriptome profiles in the tumor tissue of different genotype mice. We microscopically confirmed that the tumor tissues used to prepare RNA samples were composed of more than 80% tumor cells. Using a median fold difference test followed by FDR correction (see details in Methods), we identified 2152, 2685, and 2683 differentially expressed genes (DEGs) with FDR < 0.05 and fold change 2 by comparing RNAseq samples between $R26^{hAR/+}$:Osr1-Cre or $p53^{L/L}/R26^{hAR/+}$:Osr1-Cre versus wildtype, and $p53^{L/L}/R26^{hAR/+}$:Osr1-Cre versus $R26^{hAR/+}$:Osr1-Cre mice, respectively (Fig. 5A and Supplemental Table 4). To assess transgenic AR-mediated transcription, we compared gene sets of $R26^{hAR/+}$:Osr1-Cre and $p53^{L/L}/R26^{hAR/+}$:Osr1-Cre versus wild type mice and identified a group of overlapping DEGs (n=920) between these two groups. We also identified 1,329 DEGs related to *Trp53* deletion in comparing the gene sets of $p53^{L/L}/R26^{hAR/+}$:Osr1-Cre versus $R26^{hAR/+}$:Osr1-Cre mice. GSEA analyses with hallmark gene sets revealed eight signaling pathways based on significant enrichment in DEGs of $R26^{hAR/+}$:Osr1-Cre or $p53^{L/L}/R26^{hAR/+}$:Osr1-Cre versus wild type mice (Fig. 5B and Supplemental Fig 4). While E2F mediated signaling and G2/M checkpoint gene sets were

enriched in both the DEGs of *R26^{hAR/+}:Osr1-Cre* or *p53^{L/L}/R26^{hAR/+}:Osr1-Cre* versus wild type mice, cell signaling pathways related to tumor progression, including angiogenesis, epithelial mesenchymal transition (EMT), hypoxia, and IL6-JAK-STAT3, were only enriched in DEGs of the compound mice versus wild type mice. There was a large group of overlapping DEGs between samples of *p53^{L/L}/R26^{hAR/+}:Osr1-Cre* versus wild type or *R26^{hAR/+}:Osr1-Cre* mice (Fig. 5C and Supplemental Table 4). GSEA analyses of these DEGs showed a similar enrichment of cell signaling pathways related to tumor progression as shown above (Fig. 5D). These data indicate a role for p53 deletion in promoting prostatic tumor progression and aggressiveness.

Loss of p53 combined with transgenic AR expression induces prostatic basaloid cell tumor development

Analyses of human prostate cancer samples have shown unique molecular signatures in different types of tumor cells [24, 25]. Prostate Cancer Subtype (PCS) and PAM50 intrinsic subtyping methods have categorized human prostate cancer as luminal or basal cell tumors [24, 25]. Given the unique basaloid and squamous cell property of prostate tumors that were observed in *p53^{L/L}/R26^{hAR/+}:Osr1-Cre* and *p53^{L/+}/R26^{hAR/+}:Osr1-Cre* compound mice, we assessed if the upregulated genes in *p53^{L/L}/R26^{hAR/+}:Osr1-Cre* versus *R26^{hAR/+}:Osr1-Cre* are enriched in one of the above human PCS or PAM50 subtype tumors. Strikingly, a significant enrichment of the upregulated genes was observed in signature genes of PCS3 and Basal subtype tumors while only native enrichment showed with other subtype tumors (Fig. 6A and Supplemental Fig 5). Both of the above subtypes were characterized as human prostatic basal cell carcinomas [24, 25]. An upregulation of basal cell signature genes, including *Acta2, Gstp1, Krt5, and Trp63* was revealed within the DEGs of *p53^{L/L}/R26^{hAR/+}:Osr1-Cre* compound mice versus *R26^{hAR/+}:Osr1-Cre* mice (Fig. 6B). Increased expression of prostatic basal epithelial cell markers, *Trp63, Krt5, and Krt14*, was also shown in tumor tissues of *p53^{L/L}/R26^{hAR/+}:Osr1-Cre* using qPCR (Fig. 6C and Supplemental table 3). IHC analyses further demonstrated elevated expression of both p63 and CK5 in prostatic tumor lesions of the compound mice (Fig 6E–E" and 6D–D" and supplemental table 2). These results are consistent with our previous observation (Fig. 4), and demonstrate that loss of p53 and elevated *AR* expression promotes prostatic basal cell tumor development.

Elevated SOX2 expression and activation in prostate tumors of AR transgenic and Trp53 deletion compound mice

To assess the molecular mechanism for prostatic basal cell tumor development, we performed master regulator analysis to identify the potential regulators in *p53^{L/L}/R26^{hAR/+}:Osr1-Cre* compound mouse tumors. We identified eight transcription factors that are directly related to *Trp53* deletion based on DEGs of *p53^{L/L}/R26^{hAR/+}:Osr1-Cre* versus *R26^{hAR/+}:Osr1-Cre* mice (p < 0.01) (Fig. 7A and Supplemental Table 5). Interestingly, more than 20 genes identified in the PCS3 subtype [24] are also the downstream targets of three transcription regulators, including SOX2, SUZ12, and MTF2 (Fig. 7A), suggesting a critical role of these master regulators in basal cell tumor development. Moreover, many downstream targets of these three transcriptional factors overlap with the DEGs of *p53^{L/L}/R26^{hAR/+}:Osr1-Cre* versus *R26^{hAR/+}:Osr1-Cre* mouse samples, resulting in generating six signaling pathways in GSEA analyses (Fig. 7B and Supplemental Table 6).

Using the PCTA database, we assessed the correlation of transcription factor expression levels and the disease stages. Two tailed one-way ANOVA test revealed that the top 3 TFs' expression levels are significantly varied from benign to metastatic castration-resistant prostate cancer, mCRPC (Fig. 7C). Of note, a subset of human mCRPC shows very high expression of these TFs in comparison with primary tumors. To determine the potential roles of these TFs in the prostate tumors of $p53^{L/L}/R26^{hAR/+}$:Osr1-Cre mice, we assessed their expression using qPCR approaches. An increase in the gene expression of the top 3 TFs, including *Sox2*, *Suz12* and *Mtf2*, was observed in tumor samples of $p53^{L/L}/R26^{hAR/+}$:Osr1-Cre compound mice in comparison with $R26^{hAR/+}$:Osr1-Cre only mice (Fig. 7D). Given the recent studies that showed SOX2 plays a role in driving lineage plasticity of luminal cells to differentiate into a basal and squamous cell phenotype [8, 26], we further investigated whether SOX2 functions as a transcriptional regulator in the tumor cells of the above mice. IHC analyses showed significantly elevated expression of SOX2 in tumor cells of $p53^{L/L}/R26^{hAR/+}$-Osr1-Cre compound mice but not in tumor cells of $R26^{hAR/+}$:Osr1-Cre mice (Fig. 7F–F' versus 7E–E'). We then assessed the activity of SOX2 by examining the expression of the SOX2 downstream target genes. A significant increase of *Cav1*, *Datc3*, *Cxcl12*, *Mesi2*, *Efemp1*, and *Gas1* expression was revealed in tumor samples of $p53^{L/L}/R26^{hAR/+}$:Osr1-Cre mice in comparison with those of $R26^{hAR/+}$:Osr1-Cre mice (Fig. 7G). Interestingly, these downstream targets have also been identified within the PCS3 subtype of human prostate cancer [24] (Supplemental Table 7). Using chromatin immunoprecipitaion (ChIP) analyses, we examined the occupancy of SOX2 on their target genes. We observed significant recruitment of SOX2 within the promoter regions of both *Efemp1* and *Gas1* in tumor samples of $p53^{L/L}/R26^{hAR/+}$:Osr1-Cre compound mice in comparison with those from $R26^{hAR/+}$:Osr1-Cre only mice (Fig. 7H). Interestingly, the recruitment of SOX2 was also revealed within the enhancer regions of *Trmpss2* and *Nkx3.1* [27], the AR target genes but not the locus of *Untr4* used as a negative control [28]. To examine the potential interaction between SOX2 and AR mediated regulation, we examined the recruitment of AR in the above regulator loci. While a specific recruitment of AR was revealed in both the *Trmpss2* and *Nkx3.1* loci in tumor tissues of $R26^{hAR/+}$:Osr1-Cre and $p53^{L/L}/R26^{hAR/+}$:Osr1-Cre mice, the occupancy of AR was also observed in the regulatory regions of *Efemp1* and *Gas1* in the tumor tissues of $p53^{L/L}/R26^{hAR/+}$:Osr1-Cre mice. Taken together, the above data demonstrate the critical role of SOX2 in regulating prostatic basal cell tumor initiation, aggressiveness, and progression in *AR* transgenic and *Trp53* deletion compound mice.

DISCUSSION

The human prostate cancer genomic analyses showed that the aberrant alteration of AR and *TP53* are prevalent in advanced prostate cancers [5, 6] (Supplemental Fig. 6). Specifically, genetic alterations of *TP53* and amplification of *AR* are frequently observed in castration resistant prostate cancer CRPC [6, 17]. Clinical observations that genetic alterations of *TP53* occurs more frequently in advanced, recurrent, and metastatic prostate cancers further suggest the critical role of p53 in promoting prostate cancer progression [6]. However, the biological effect of *AR* amplification and p53 loss in prostate tumorigenesis is largely unknown. In addition, there is limited knowledge regarding the molecular mechanism underlying these dual genetic modifications in prostate tumorigenesis. In this study, we

generated $p53^{L/+}/R26^{hAR/+}$:Osr1-Cre and $p53^{L/L}/R26^{hAR/+}$:Osr1-Cre compound mice, in which induced *AR* transgene and reduced or loss of *Trp53* expression simultaneously occur within the mouse prostate epithelium. These mouse models mimic what happens in human prostate cancer cells and allow us to directly assess the collaborative role of AR and p53 abnormalities in prostate tumorigenesis. We observed an earlier onset of oncogenic transformation, an accelerated tumor development, and aggressive tumor phenotypes in the prostate of the compound mice in comparison with *AR* transgenic only mice [3]. Of note, the prostatic tumors in both AR transgenic and compound mice were regressed after castration, indicating that they are androgen responsive. Interestingly, either heterozygous or homozygous deletion of *Trp53* in mouse prostatic epithelium did not result in any visible pathological changes in this study. The aggressive tumor phenotypes of $p53^{L/+}/R26^{hAR/+}$:Osr1-Cre and $p53^{L/L}/R26^{hAR/+}$:Osr1-Cre compound mice are consistent with previous clinical observations and recapitulate the biological consequence of aberrant AR and p53 deletion in tumor development and progression.

Histological analyses showed typical pathological changes resembling basaloid carcinomas with massive squamous differentiation in prostate tumors of all of the $p53^{L/+}/R26^{hAR/+}$:Osr1-Cre and $p53^{L/L}/R26^{hAR/+}$:Osr1-Cre compound mice. These diverse and aggressive malignant characteristics reflect the heterogenic nature of those prostate tumors. In addition, the development of aggressive tumor phenotypes in the compound mice demonstrates the promotional role of the dual genetic alteration in AR and p53 pathways in prostatic tumor development and progression. The divergence of the different tumor types in the compound mice suggests that oncogenic transformation may have initiated from different cells of origin. Both prostatic luminal and basal epithelial cells have been shown to possess the ability to initiate oncogenic transformation and can function as tumor initiating cells [29]. IHC analyses showed predominant atypical cells with CK5 and transgenic AR positive staining within PIN lesions of the compound mice. Strong staining of transgenic AR, loss of staining for luminal cell marker CK8, and increased staining of basal cell markers p63, CK5, were further revealed in most prostatic tumor cells in the compound mice. These results suggest those atypical cells possessing basal cell properties could further progress and develop more aggressive tumor types in the compound mice bearing transgenic AR expression with either homozygous or heterozygous *Trp53* deletion. Interestingly, the deletion of p53 has been shown to induce the lineage plasticity of prostate cancer from a luminal-like carcinoma to basal-like carcinoma [30]. In addition, genetic induction of tumorigenesis originated from basal cells can also develop squamous cell carcinoma [31]. Since only prostatic adenocarcinomas were developed in *AR* transgenic mice [3], these lines of evidence suggest an important role of p53 in maintaining cell differentiation and lineages, and thus reduction and loss of p53 will promote tumor cell trans-differentiation and induce disease progression.

To delineate the molecular basis underlying elevated AR expression and p53 loss in prostate tumorigenesis, we performed RNA-sequencing using tumor samples isolated from different genotypes of mice. Strikingly, RNA-seq transcriptome profiling analysis showed a significant enrichment of prostate basal cell subtypes (PAM50) and PCS3 (PCS) in the prostatic tissues isolated from $p53^{L/+}/R26^{hAR/+}$:Osr1-Cre and $p53^{L/L}/R26^{hAR/+}$:Osr1-Cre compound mice [24, 25]. GSEA analyses showed significant enrichment in angiogenesis, EMT,

hypoxia, and IL6-JAK-STAT3 mediated signaling pathways in tumor cells of the compound mice. These data provide the molecular basis for p53 loss-induced prostatic basal cell carcinoma formation and disease progression. Using Master Regulator Analysis analytic tools, we further identified the potential master regulators that may directly contribute to the aggressive tumor phenotypes as observed in the compound mice. SRY (sex determining region Y)-box2 gene (SOX2) appeared as the top candidate on the list (Fig.6A). SOX2 is a transcription factor and a member of the SOX family [32]. It is essential for maintaining the status of undifferentiated embryonic stem cells. The focal expression of SOX2 appeared within the basal cell layer of the prostate glands [33]. Interestingly, increased SOX2 expression has also been observed in enzalutamide-resistant prostate cancer cells bearing both TP53 and RB1 loss [30]. These data suggest an important role of SOX2 in prostate cancer progression.

Given the clinical relevance of SOX2 in advanced prostate cancer, we assessed the expression and activity of SOX2 in prostatic tumor cells in the AR transgenic and p53 deletion mice. Elevated expression of SOX2 was revealed specifically in tumor cells of the compound mice. Increased expression of SOX2 downstream target genes was also observed in tumor tissues isolated from the compound mice in comparison to samples from AR transgenic mice. Interestingly, it was also shown an overlap between the target genes of SOX2 and the signature genes from PCS3 subtype [24]. Using ChIP assays, we directly examined the regulatory role of SOX2 in prostatic basal tumor development. An extensive recruitment of SOX2 was detected in the regulatory loci of the both *Efemp* and *Gas1* genes in tumor samples isolated from the compound mice in comparison with AR transgenic mice. Interestingly, in the above ChIP assays, we also observed the recruitment of SOX2 on the regulatory loci of the AR target genes, *Trmpss2* and *Nkx3.1*. To determine a potential interaction between the AR and SOX2, we examined the role of AR in regulating those SOX2 target genes. Intriguingly, an extensive occupancy of AR was detected on the regulator loci of the both AR downstream targets, *Trmpss2 and Nkx3.1,* as well as SOX2 target genes, *Efemp* and *Gas1,* in the tumor samples of the compound mice. These results implicate a co-occupancy of AR and SOX2 on the regulatory regions of their target genes, and elucidate a novel molecular mechanism by which AR and SOX2 collaboratively regulate prostate cancer cell trans-differentiation and disease progression in tumor tissues of the compound mice bearing upregulated AR expression and loss of or reduced p53 expression.

MATERIALS AND METHODS

Mouse mating and genotyping

All mice used in this study were from a C57BL/6 background. The *Trp53* floxed mice, *p53^{LoxP/LoxP}* mice, also named *p53^{L/L}*, were obtained from Jackson Laboratory (stock: 008462). The *AR* transgenic mouse, *R26hAR^{LoxP/wt}*, also named *R26^{hAR/+}*, was generated as described previously [3]. *Osr1-Cre* mice were kindly provided by Dr. Gail Martin [20]. Either *p53^{L/+}:R26^{hAR/+}* or *p53^{L/+}:Osr1-Cre* mice were first generated and then used to produce *p53^{L/L}:Osr1-Cre, p53^{L/+}:Osr1-Cre, R26^{hAR/+}:Osr1-Cre, p53^{L/+}/R26^{hAR/+}:Osr1-Cre* and *p53^{L/L}/R26^{hAR/+}:Osr1-Cre* mice. Mice were genotyped by PCR using specific primers for detecting either *AR* or *trp53* targeted or deleted alleles (Supplemental table 1) [3, 34, 35]. All animal experiments performed in this study were approved by the ethics committee of the

Administrative Panel on Institutional Animal Care and Use Committee at Stanford University and Beckman Research Institute/City of Hope.

Pathological analyses

In this study, the guidelines recommended by The Mouse Models of Human Cancers Consortium Prostate Pathology Committee in 2013 were used for the pathological analyses [21]. Mouse tissues were processed and Hematoxylin-eosin staining (H&E) was performed as described previously [3].

Immunohistochemistry (IHC)

IHC was performed as previously described [3]. Tissue sections were treated by boiling in 0.01 M Citrate buffer (pH 6.0) for antigen retrieval, blocked in 5% normal goat serum, and incubated with primary antibodies diluted in 1% normal goat serum at 4°C overnight (Supplemental Table 2 for the antibody information). Slides were incubated with biotinylated secondary antibodies for 1 hour then with horseradish peroxidase streptavidin (SA-5004, Vector Laboratories, Burlingame, CA, USA) for 30 min, visualized by DAB kit (SK-4100, Vector Laboratories), then counterstained with 5% (w/v) Harris Hematoxylin, and subsequently mounted with Permount Mounting Medium (SP15–500, Thermo Fisher Scientific, Waltham, MA, USA).

Microscope image acquisition

Images of H&E and immunohistochemistry were acquired on an Axio Lab. A1 microscope using 10x and 40x Zeiss A-Plan objectives with a Canon EOS 1000D camera and using Axiovision software (Carl Zeiss, Oberkochen, Germany).

RNA isolation, reverse transcription (RT)-Quantitative PCR (RT-qPCR), and RNA sequencing

RNA samples were isolated from fresh mouse tissues using RNA-Bee (TEL-TEST, Inc., Friendswood, TX, USA) or from formalin-fixed Paraffin Embedded (FFPE) slides using the Pinpoint Side RNA isolation Kit (Zymo Research, Cat R1007). RNA sequencing libraries were prepared with Kapa RNA HyperPrep Kit with RiboErase (Kapa Biosystems, Cat KR1351). Sequencing runs were performed on Illumina Hiseq 2500 in the single read mode of 51 cycles of read 1 and 7 cycles of index with V4 Kits. Real-time analysis (RTA) 2.2.38 software was used to process the image analysis and base calling. Reverse transcription was performed as described previously [36], and RT-qPCR assays were carried out using SYBR GreenER qPCR Super Mix Universal (11762, Invitrogen) with specific primers (Supplemental Table 3) on the 7500 Real-Time PCR system (Thermo Fisher Scientific).

Chromatin immunoprecipitation (ChIP) Assays

ChIP assays were performed as described previously [37]. Briefly, mouse tissues were minced and incubated with 1% formaldehyde for 15 min and quenched with 0.150 M glycine for 10 min. Samples were washed sequentially with cold PBS, and resuspended in cell lysis buffer (50 mM Tris-HCl (pH 8.0), 140 mM NaCl, 1 mM EDTA, 10% Glycerol, 0.5% NP-40, and 0.25% Triton X-100), and then homogenized. The chromatin was sheared in nuclear lysis

buffer (10 mM Tris-HCl, pH 8.0, 1 mM EDTA, 0.5 mM EGTA, and 0.2% SDS) to an average size of 200–500 bp by sonication, and then diluted 3-fold in ChIP dilution buffer (0.01% SDS, 1.1% Triton X-100, 1.2 mM EDTA, 16.7 mM Tris-HCl, pH 8.1, and 167 mM NaCl), and was subjected to immunoprecipitation by magnetic protein G beads (Invitrogen) conjugated with AR (ab74272, abcam) or SOX2 antibody (39843, Active Motif). Cross-links were reversed and chromatin DNA fragments were analyzed by real-time qPCR with specific primers (Supplemental Table 3).

Data preprocessing, normalization, and analyses

Quality of sequencing data was verified using MultiQC software [38]. Sequence alignment and quantification were performed using the STAR-RSEM pipeline [39]. Reads overlapping exons in the annotation of Genome Reference Consortium Mouse Build 38 (GRCm38) were identified, and would be excluded from further downstream analysis if they failed to achieve raw read counts of at least 2 across all the libraries. The trimmed mean of M-values normalization method (TMM) [40] (version 1.6.1) was used for calculating normalized count data. Three comparisons were performed between prostate tissues of different genotype mice using median difference test in this study [41]. For each gene, a P-value was computed by performing a two-tailed median difference test using the empirical distributions that were estimated by random permutations of the samples. Multiple testing correction was done by using Storey's correction method [42]. The differentially expressed genes (DEGs) were selected as those having false discovery rate (FDR) < 0.05 and fold-change > 2. The enriched gene sets represented by DEGs were identified as the hallmark gene sets [43] having nominal $P < 0.05$ from gene set enrichment analysis (GSEA) [44]. GSEA was performed using the Prostate Cancer Transcriptome Atlas (PCTA: www.thepcta.org), which contains 1,321 human prostate cancer transcriptome profiles categorized based on Prostate Cancer Subtype (PCS) [24] and the PAM50 scheme [25]. DEGs from mouse tumor samples were ranked by fold change between groups and compared to the PCTA prostate cancer subtypes. To identify the potential master transcriptional regulators, we made a compendium of transcription factors (TF) based on their target genes that were collected from different genome-wide ChIP databases, including ChIPBase [45], Amadeus [46], hmChIP [47], ChEA [48], CellNet [49], and MSigDB [50]. The target genes for TF were identified from the DEGs, which were then randomly sampled from the whole genome. The above measurement was repeated 100,000 times to generate an empirical null hypothesis. The significance level (P-value) of the TF-target relationships in the DEGs was computed using a one-tailed test with the empirical null hypothesis. The similar analysis was performed for all TFs, and significant TFs were selected with P-value < 0.01.

Statistical Analysis

Principal component analysis (PCA) was used for visualization and to assess sample distribution by gene expression profile, and the MATLAB (v.9.0; Mathworks, Natick, MA, USA), the R (v.3.5) and Python (v.3.7) were used for bioinformatics analysis.

Supplementary Material

Refer to Web version on PubMed Central for supplementary material.

Acknowledgements

References

1. Kyprianou N, Isaacs JT. Activation of programmed cell death in the rat ventral prostate after castration. Endocrinology 1988; 122: 552–562. [PubMed: 2828003]

2. Huggins C, Hodges CV. Studies on prostatic cancer: I. The effect of castration, of estrogen and of androgen injection on serum phosphatases in metastatic carcinoma of the prostate. 1941. J Urol 2002; 168: 9–12. [PubMed: 12050481]

3. Zhu C, Luong R, Zhuo M, Johnson DT, McKenney JK, Cunha GR et al. Conditional expression of the androgen receptor induces oncogenic transformation of the mouse prostate. J Biol Chem 2011; 286: 33478–33488. [PubMed: 21795710]

4. Heinlein CA, Chang C. Androgen receptor in prostate cancer. Endocr Rev 2004; 25: 276–308. [PubMed: 15082523]

5. Robinson D, Van Allen EM, Wu YM, Schultz N, Lonigro RJ, Mosquera JM et al. Integrative clinical genomics of advanced prostate cancer. Cell 2015; 161: 1215–1228. [PubMed: 26000489]

6. Quigley DA, Dang HX, Zhao SG, Lloyd P, Aggarwal R, Alumkal JJ et al. Genomic Hallmarks and Structural Variation in Metastatic Prostate Cancer. Cell 2018; 174: 758–769.e759. [PubMed: 30033370]

7. Koivisto P, Kononen J, Palmberg C, Tammela T, Hyytinen E, Isola J et al. Androgen receptor gene amplification: a possible molecular mechanism for androgen deprivation therapy failure in prostate cancer. Cancer Res 1997; 57: 314–319. [PubMed: 9000575]

8. Aggarwal R, Huang J, Alumkal JJ, Zhang L, Feng FY, Thomas GV et al. Clinical and Genomic Characterization of Treatment-Emergent Small-Cell Neuroendocrine Prostate Cancer: A Multi-institutional Prospective Study. J Clin Oncol 2018; 36: 2492–2503. [PubMed: 29985747]

9. Chen CD, Welsbie DS, Tran C, Baek SH, Chen R, Vessella R et al. Molecular determinants of resistance to antiandrogen therapy. Nat Med 2004; 10: 33–39. [PubMed: 14702632]

10. Takeda DY, Spisak S, Seo JH, Bell C, O'Connor E, Korthauer K et al. A Somatically Acquired Enhancer of the Androgen Receptor Is a Noncoding Driver in Advanced Prostate Cancer. Cell 2018; 174: 422–432.e413. [PubMed: 29909987]

11. Ko LJ, Prives C. p53: puzzle and paradigm. Genes Dev 1996; 10: 1054–1072. [PubMed: 8654922]

12. Bookstein R, MacGrogan D, Hilsenbeck SG, Sharkey F, Allred DC. p53 is mutated in a subset of advanced-stage prostate cancers. Cancer research 1993; 53: 3369–3373. [PubMed: 8324747]

13. Kleihues P, Schauble B, zur Hausen A, Esteve J, Ohgaki H. Tumors associated with p53 germline mutations: a synopsis of 91 families. Am J Pathol 1997; 150: 1–13. [PubMed: 9006316]

14. Wang S, Gao J, Lei Q, Rozengurt N, Pritchard C, Jiao J et al. Prostate-specific deletion of the murine Pten tumor suppressor gene leads to metastatic prostate cancer. Cancer cell 2003; 4: 209–221. [PubMed: 14522255]

15. Zhou Z, Flesken-Nikitin A, Nikitin AY. Prostate cancer associated with p53 and Rb deficiency arises from the stem/progenitor cell–enriched proximal region of prostatic ducts. Cancer research 2007; 67: 5683–5690. [PubMed: 17553900]

16. Voeller HJ, Sugars LY, Pretlow T, Gelmann EP. p53 oncogene mutations in human prostate cancer specimens. J Urol 1994; 151: 492–495. [PubMed: 7904314]

17. Robinson D, Van Allen EM, Wu Y-M, Schultz N, Lonigro RJ, Mosquera J-M et al. Integrative clinical genomics of advanced prostate cancer. Cell 2015; 161: 1215–1228. [PubMed: 26000489]

18. Smith BA, Sokolov A, Uzunangelov V, Baertsch R, Newton Y, Graim K et al. A basal stem cell signature identifies aggressive prostate cancer phenotypes. Proc Natl Acad Sci U S A 2015; 112: E6544–6552. [PubMed: 26460041]

19. Cerami E, Gao J, Dogrusoz U, Gross BE, Sumer SO, Aksoy BA et al. The cBio cancer genomics portal: an open platform for exploring multidimensional cancer genomics data. Cancer Discov 2012; 2: 401–404. [PubMed: 22588877]

20. Grieshammer U, Agarwal P, Martin GR. A Cre transgene active in developing endodermal organs, heart, limb, and extra-ocular muscle. Genesis 2008; 46: 69–73. [PubMed: 18257103]

21. Ittmann M, Huang J, Radaelli E, Martin P, Signoretti S, Sullivan R et al. Animal models of human prostate cancer: the consensus report of the New York meeting of the Mouse Models of Human Cancers Consortium Prostate Pathology Committee. Cancer Res 2013; 73: 2718–2736. [PubMed: 23610450]

22. Zhou Z, Flesken-Nikitin A, Corney DC, Wang W, Goodrich DW, Roy-Burman P et al. Synergy of p53 and Rb deficiency in a conditional mouse model for metastatic prostate cancer. Cancer research 2006; 66: 7889–7898. [PubMed: 16912162]

23. Frohwitter G, Buerger H, VAND PJ, Korsching E, Kleinheinz J, Fillies T. Cytokeratin and protein expression patterns in squamous cell carcinoma of the oral cavity provide evidence for two distinct pathogenetic pathways. Oncol Lett 2016; 12: 107–113. [PubMed: 27347109]

24. You S, Knudsen BS, Erho N, Alshalalfa M, Takhar M, Al-Deen Ashab H et al. Integrated Classification of Prostate Cancer Reveals a Novel Luminal Subtype with Poor Outcome. Cancer Res 2016; 76: 4948–4958. [PubMed: 27302169]

25. Zhao SG, Chang SL, Erho N, Yu M, Lehrer J, Alshalalfa M et al. Associations of Luminal and Basal Subtyping of Prostate Cancer With Prognosis and Response to Androgen Deprivation Therapy. JAMA Oncol 2017; 3: 1663–1672. [PubMed: 28494073]

26. Mollaoglu G, Jones A, Wait SJ, Mukhopadhyay A, Jeong S, Arya R et al. The Lineage-Defining Transcription Factors SOX2 and NKX2–1 Determine Lung Cancer Cell Fate and Shape the Tumor Immune Microenvironment. Immunity 2018; 49: 764–779.e769. [PubMed: 30332632]

27. Chen Y, Chi P, Rockowitz S, Iaquinta PJ, Shamu T, Shukla S et al. ETS factors reprogram the androgen receptor cistrome and prime prostate tumorigenesis in response to PTEN loss. Nat Med 2013; 19: 1023–1029. [PubMed: 23817021]

28. Wyce A, Bai Y, Nagpal S, Thompson CC. Research Resource: The androgen receptor modulates expression of genes with critical roles in muscle development and function. Mol Endocrinol 2010; 24: 1665–1674. [PubMed: 20610535]

29. Matusik RJ, Jin RJ, Sun Q, Wang Y, Yu X, Gupta A et al. Prostate epithelial cell fate. Differentiation 2008; 76: 682–698. [PubMed: 18462434]

30. Mu P, Zhang Z, Benelli M, Karthaus WR, Hoover E, Chen CC et al. SOX2 promotes lineage plasticity and antiandrogen resistance in TP53- and RB1-deficient prostate cancer. Science 2017; 355: 84–88. [PubMed: 28059768]

31. Stoyanova T, Cooper AR, Drake JM, Liu X, Armstrong AJ, Pienta KJ et al. Prostate cancer originating in basal cells progresses to adenocarcinoma propagated by luminal-like cells. Proc Natl Acad Sci U S A 2013; 110: 20111–20116. [PubMed: 24282295]

32. Sarkar A, Hochedlinger K. The sox family of transcription factors: versatile regulators of stem and progenitor cell fate. Cell Stem Cell 2013; 12: 15–30. [PubMed: 23290134]

33. Esposito S, Russo MV, Airoldi I, Tupone MG, Sorrentino C, Barbarito G et al. SNAI2/Slug gene is silenced in prostate cancer and regulates neuroendocrine differentiation, metastasis-suppressor and pluripotency gene expression. Oncotarget 2015; 6: 17121–17134. [PubMed: 25686823]

34. Johnson DT, Luong R, Lee SH, Peng Y, Shaltouki A, Lee JT et al. Deletion of leucine zipper tumor suppressor 2 (lzts2) increases susceptibility to tumor development. J Biol Chem 2013; 288: 3727–3738. [PubMed: 23275340]

35. Kwak MK, Johnson DT, Zhu C, Lee SH, Ye DW, Luong R et al. Conditional deletion of the Pten gene in the mouse prostate induces prostatic intraepithelial neoplasms at early ages but a slow progression to prostate tumors. PLoS One 2013; 8: e53476. [PubMed: 23308230]

36. Lee SH, Luong R, Johnson DT, Cunha GR, Rivina L, Gonzalgo ML et al. Androgen signaling is a confounding factor for beta-catenin-mediated prostate tumorigenesis. Oncogene 2016; 35: 702–714. [PubMed: 25893287]

37. Lee J, Beliakoff J, Sun Z. The novel PIAS-like protein hZimp10 is a transcriptional co-activator of the p53 tumor suppressor. Nucleic Acids Res 2007; 35: 4523–4534. [PubMed: 17584785]

38. Ewels P, Magnusson M, Lundin S, Kaller M. MultiQC: summarize analysis results for multiple tools and samples in a single report. Bioinformatics 2016; 32: 3047–3048. [PubMed: 27312411]

39. Chamarthy MR, Williams SC, Moadel RM. Radioimmunotherapy of non-Hodgkin's lymphoma: from the 'magic bullets' to 'radioactive magic bullets'. Yale J Biol Med 2011; 84: 391–407. [PubMed: 22180677]

40. Robinson MD, Oshlack A. A scaling normalization method for differential expression analysis of RNA-seq data. Genome Biol 2010; 11: R25. [PubMed: 20196867]

41. You S, Yoo SA, Choi S, Kim JY, Park SJ, Ji JD et al. Identification of key regulators for the migration and invasion of rheumatoid synoviocytes through a systems approach. Proc Natl Acad Sci U S A 2014; 111: 550–555. [PubMed: 24374632]

42. Storey JD. A Direct Approach to False Discovery Rates. Journal Of The Royal Statistical Society 2002; 64: 478–479.

43. Liberzon A, Birger C, Thorvaldsdottir H, Ghandi M, Mesirov JP, Tamayo P. The Molecular Signatures Database (MSigDB) hallmark gene set collection. Cell Syst 2015; 1: 417–425. [PubMed: 26771021]

44. Subramanian A, Tamayo P, Mootha VK, Mukherjee S, Ebert BL, Gillette MA et al. Gene set enrichment analysis: a knowledge-based approach for interpreting genome-wide expression profiles. Proc Natl Acad Sci U S A 2005; 102: 15545–15550. [PubMed: 16199517]

45. Yang JH, Li JH, Jiang S, Zhou H, Qu LH. ChIPBase: a database for decoding the transcriptional regulation of long non-coding RNA and microRNA genes from ChIP-Seq data. Nucleic Acids Res 2013; 41: D177–187. [PubMed: 23161675]

46. Linhart C, Halperin Y, Shamir R. Transcription factor and microRNA motif discovery: the Amadeus platform and a compendium of metazoan target sets. Genome Res 2008; 18: 1180–1189. [PubMed: 18411406]

47. Chen L, Wu G, Ji H. hmChIP: a database and web server for exploring publicly available human and mouse ChIP-seq and ChIP-chip data. Bioinformatics 2011; 27: 1447–1448. [PubMed: 21450710]

48. Lachmann A, Xu H, Krishnan J, Berger SI, Mazloom AR, Ma'ayan A. ChEA: transcription factor regulation inferred from integrating genome-wide ChIP-X experiments. Bioinformatics 2010; 26: 2438–2444. [PubMed: 20709693]

49. Cahan P, Li H, Morris SA, Lummertz da Rocha E, Daley GQ, Collins JJ. CellNet: network biology applied to stem cell engineering. Cell 2014; 158: 903–915. [PubMed: 25126793]

50. Liberzon A, Subramanian A, Pinchback R, Thorvaldsdottir H, Tamayo P, Mesirov JP. Molecular signatures database (MSigDB) 3.0. Bioinformatics 2011; 27: 1739–1740. [PubMed: 21546393]
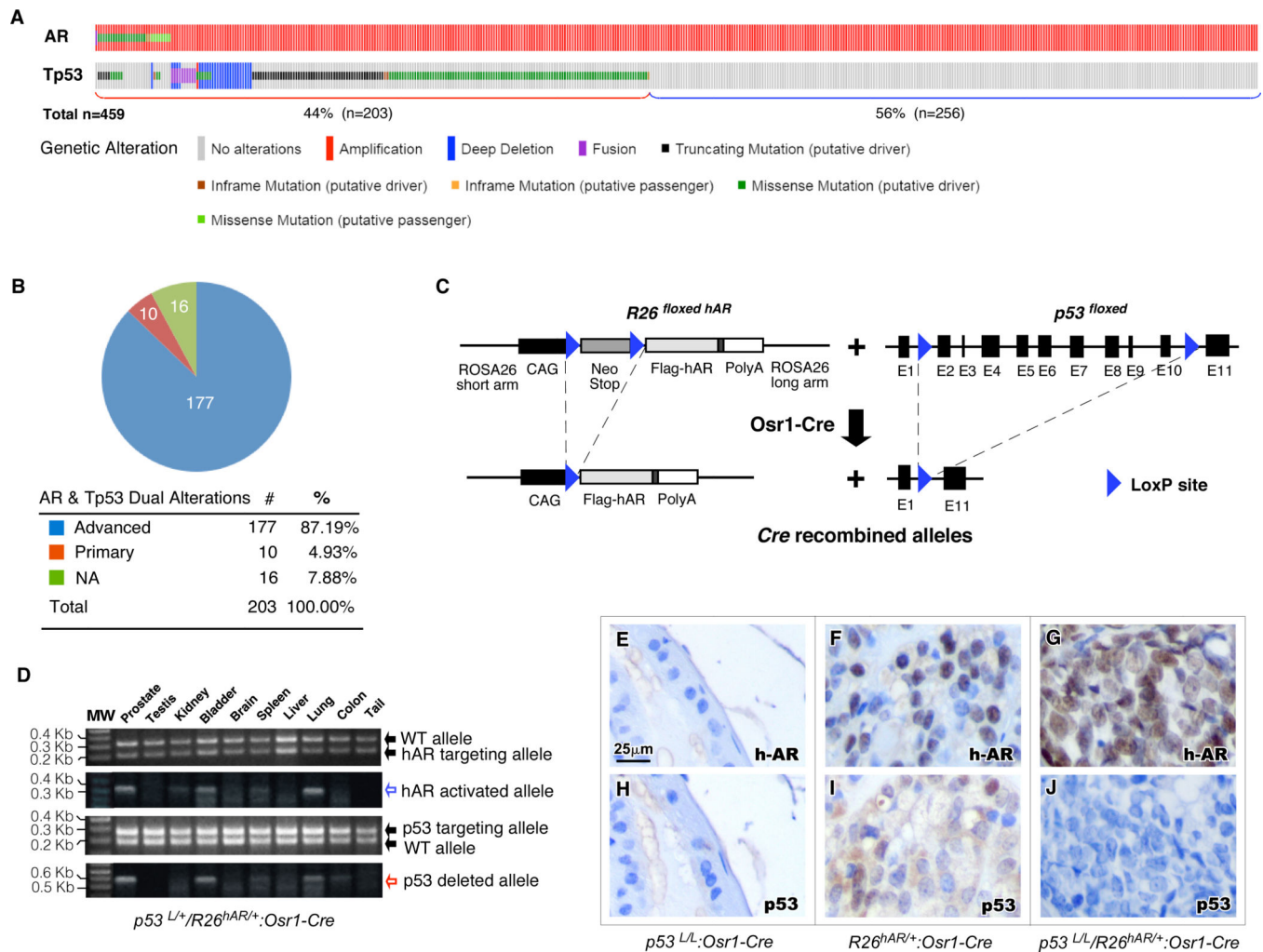
Figure 1. Generation of mouse models to mimic the co-occurrence of *AR* amplification and loss of *TP53* expression in human prostate cancer.

A. Oncoprint generated from human prostate cancer samples showing significant co-occurrence of *AR* alteration and aberration of p53 (see https://www.cbioportal.org). **B**. Percentages of advanced prostate cancer samples in the patient cohort showing alterations of both *AR* and *TP53*. **C**. Schematic of the floxed *AR* transgene and the *Trp53* deletion target constructs, as well as the corresponding recombined alleles. **D**. Representative genomic PCR results confirming the *AR* or *Trp53* targeting alleles (black solid arrows) and *AR* recombined (blue empty arrow) or *Trp53* deleted (red empty arrow) alleles from indicated mouse tissues. **E-J**. Representative immunohistochemistry (IHC) staining of prostate tissue sections from mice of the indicated genotypes. IHC staining were performed with the indicated antibodies: h-AR (**E-G**) and p53 (**H-J**) antibodies. Scale bar: 25 μm.
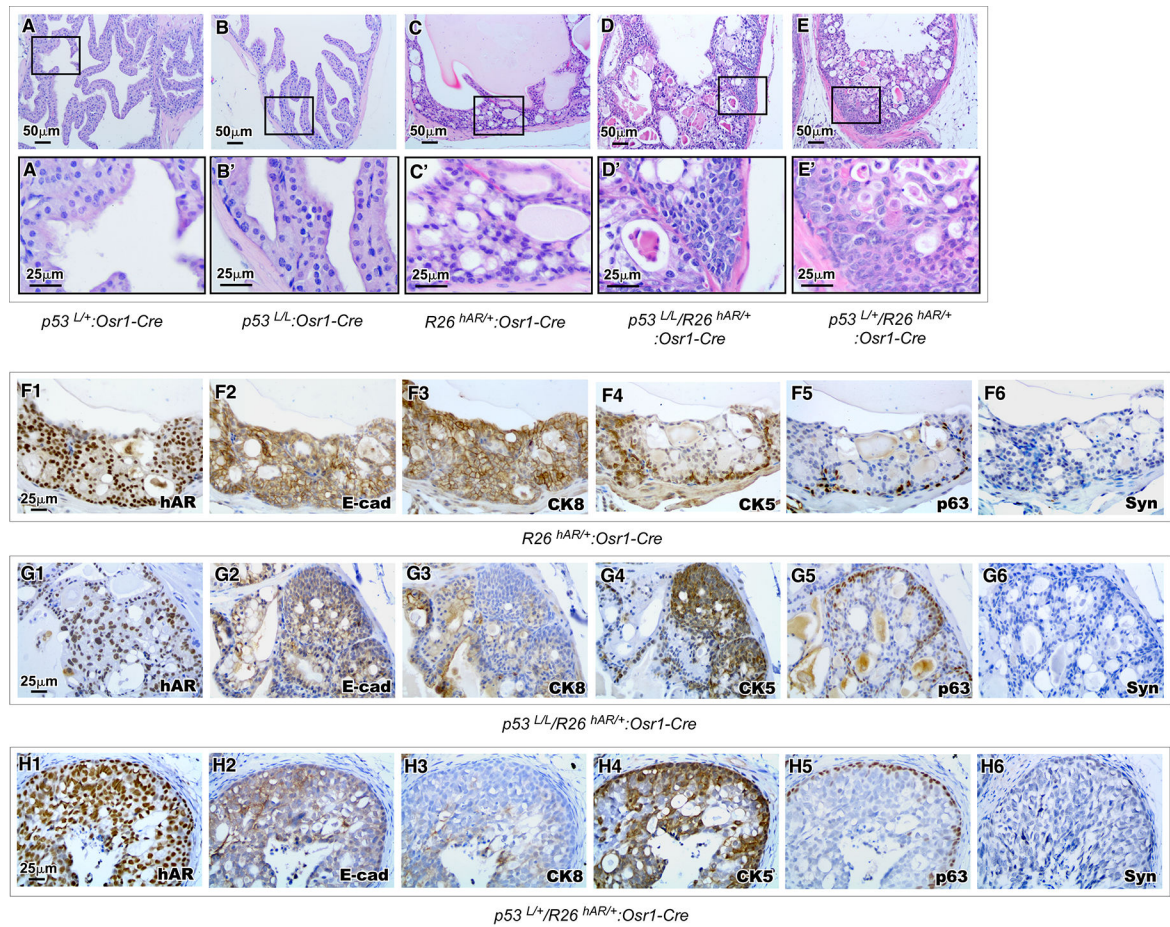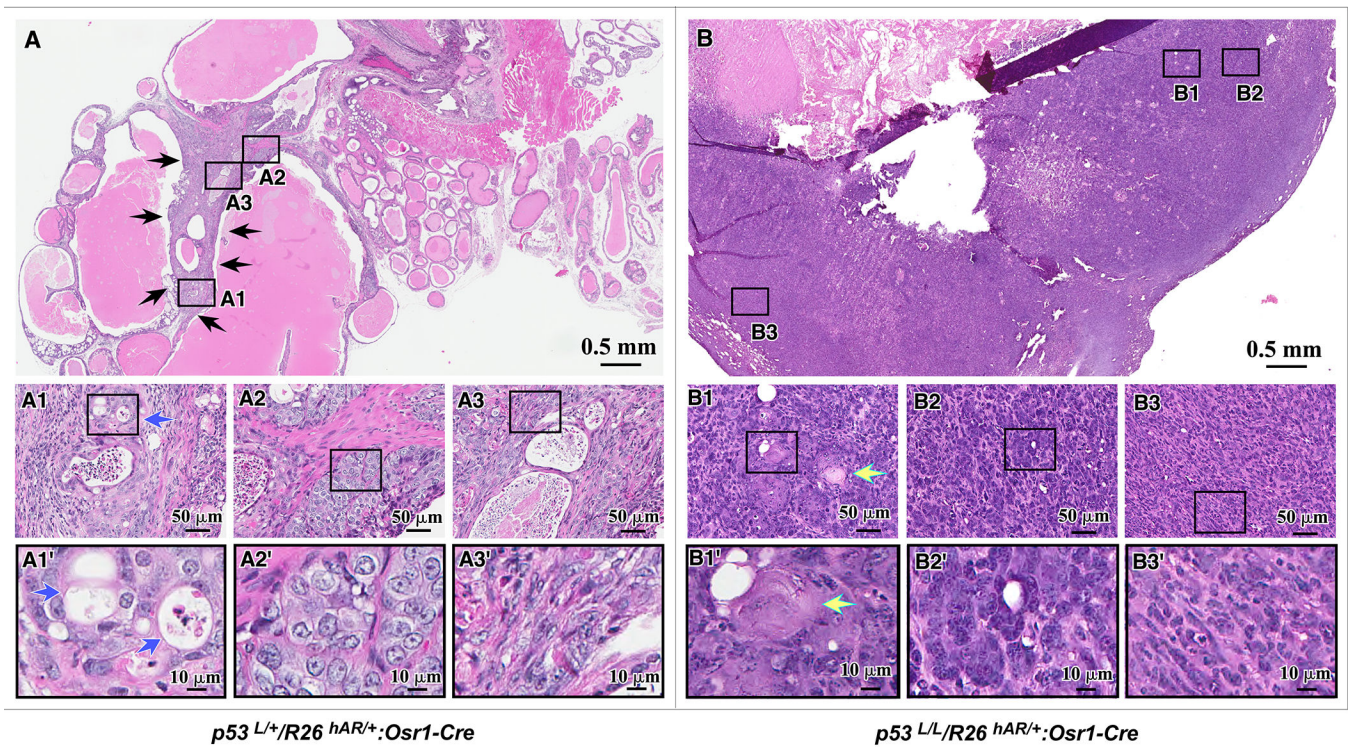
I. Pathological Abnormalities in the Prostates of p53 Knockout and AR Transgenic Mice

Genotypes	< 6 months	6 - 12 months	> 12 months
p53^{L/L}/R26^{hAR/+}:Osr1-Cre	4 in 4 LGPIN* 3 of 4 HGPIN**	6 of 6 HGPIN 4 of 6 PCa***	5 of 5 HGPIN 4 of 5 PCa
p53^{L/+}/R26^{hAR/+}:Osr1-Cre	2 of 4 LGPIN 1 of 4 HGPIN	4 of 5 HGPIN 1 of 5 PCa	7 of 7 HGPIN 5 of 7 PCa
R26^{hAR/+}:Osr1-Cre	1 of 8 LGPIN	5 of 6 LGPIN 2 of 6 HGPIN	7 of 9 HGPIN 4 of 9 PCa
p53^{L/L}:Osr1-Cre	6 of 6 normal	7 of 7 normal	7 of 7 normal
p53^{L/Wt}:Osr1-Cre	8 of 8 normal	6 of 6 normal	5 of 5 normal

*LGPIN: Low grade prostatic intraepithelial neoplasia; **HGPIN: High grade prostatic intraepithelial neoplasia;
***PCa: Prostate Cancer

Figure 2. Loss of *Trp53* enhances AR-mediated oncogenic transformation in the murine prostate.
A-E. Representative H&E stains of prostatic tissues isolated from mice of the indicated genotypes mice at three months of age. Scale bar: 50 μm (A-E); or 25 μm (A'-E'). **F-H**. Representative IHC stains of prostate tissue sections from 3 month-old mice of the indicated genotypes with antibodies as indicated above. **I**. Summary of pathological abnormalities in the prostates of *Trp53* deletion and *AR* transgenic mice.

Figure 3. Conditional expression of AR and deletion of *Trp53* in the mouse prostate accelerates prostatic tumor formation.

A. Representative H&E staining of prostatic tumor lesions from $p53^{L/+}/R26^{hAR/+}$:Osr1-Cre mice. Scale bar: 0.5mm, or 50 μm or 10 μm in magnified views. **B**. Representative H&E staining of prostatic tumor lesions from $p53^{L/L}/R26^{hAR/+}$:Osr1-Cre mice. Scale bar: 0.5mm, or 50 μm or 10 μm in magnified views. **C**. Classification of prostatic tumors in mice of the indicated genotypes.
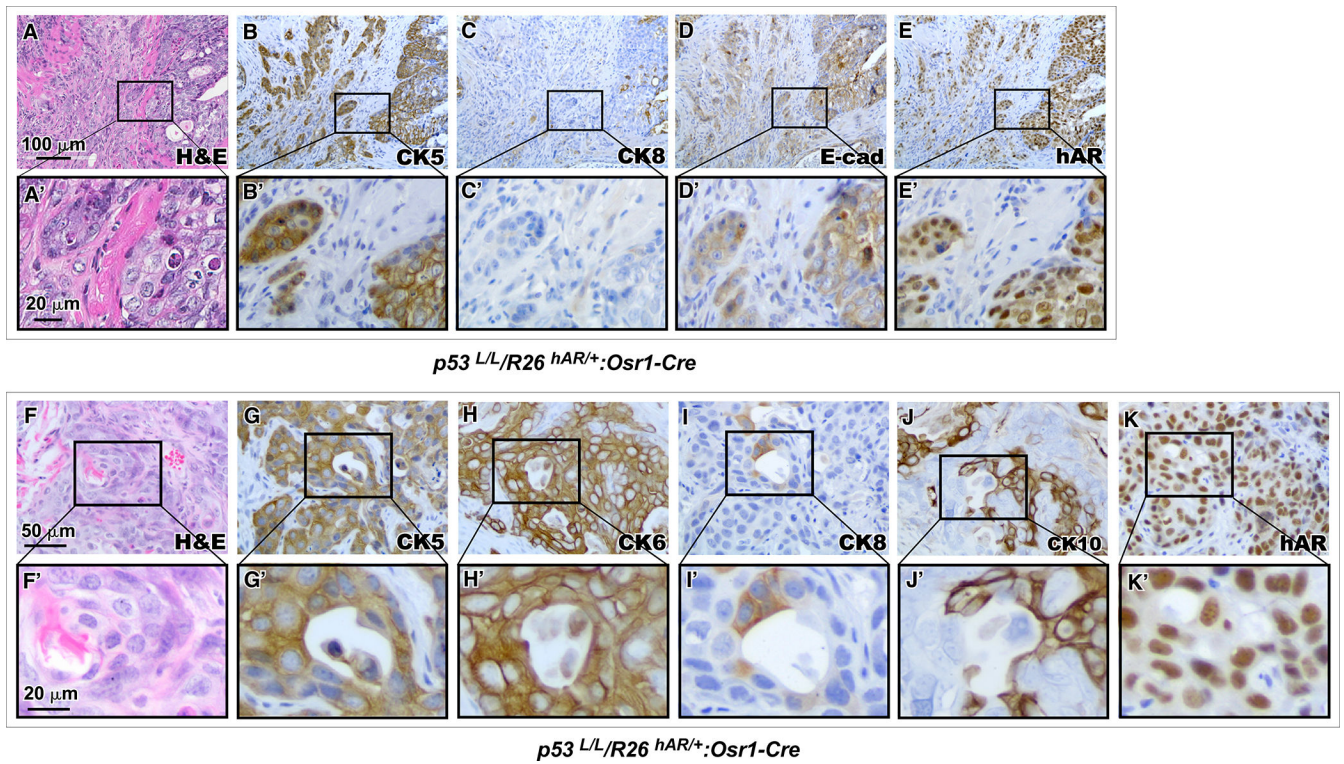
Figure 4. Basaloid and squamous prostate tumors are developed in the AR transgenic and compound mice.
A. Representative H&E staining of basaloid tumor in prostate tissues isolated from *p53^{L/L}/R26^{hAR/+}:Osr1-Cre* mice. Scale bar: 100 μm, or 20 um in magnified view. **B-E**. Representative IHC stains of prostatic basaloid tumor lesions with indicated antibodies. Scale bar: 100 μm, or 20 μm in magnified views. **F**. Representative H&E staining of adenosquamous tumor in prostate tissues from *p53^{L/L}/R26^{hAR/+}:Osr1-Cre* mice. Scale bar: 100 μm, or 20 um in magnified view. **G-K**. Similar IHC analysis as in sections B-E, with the antibodies as indicated above. Scale bar: 50 μm, or 20 μm in magnified views.
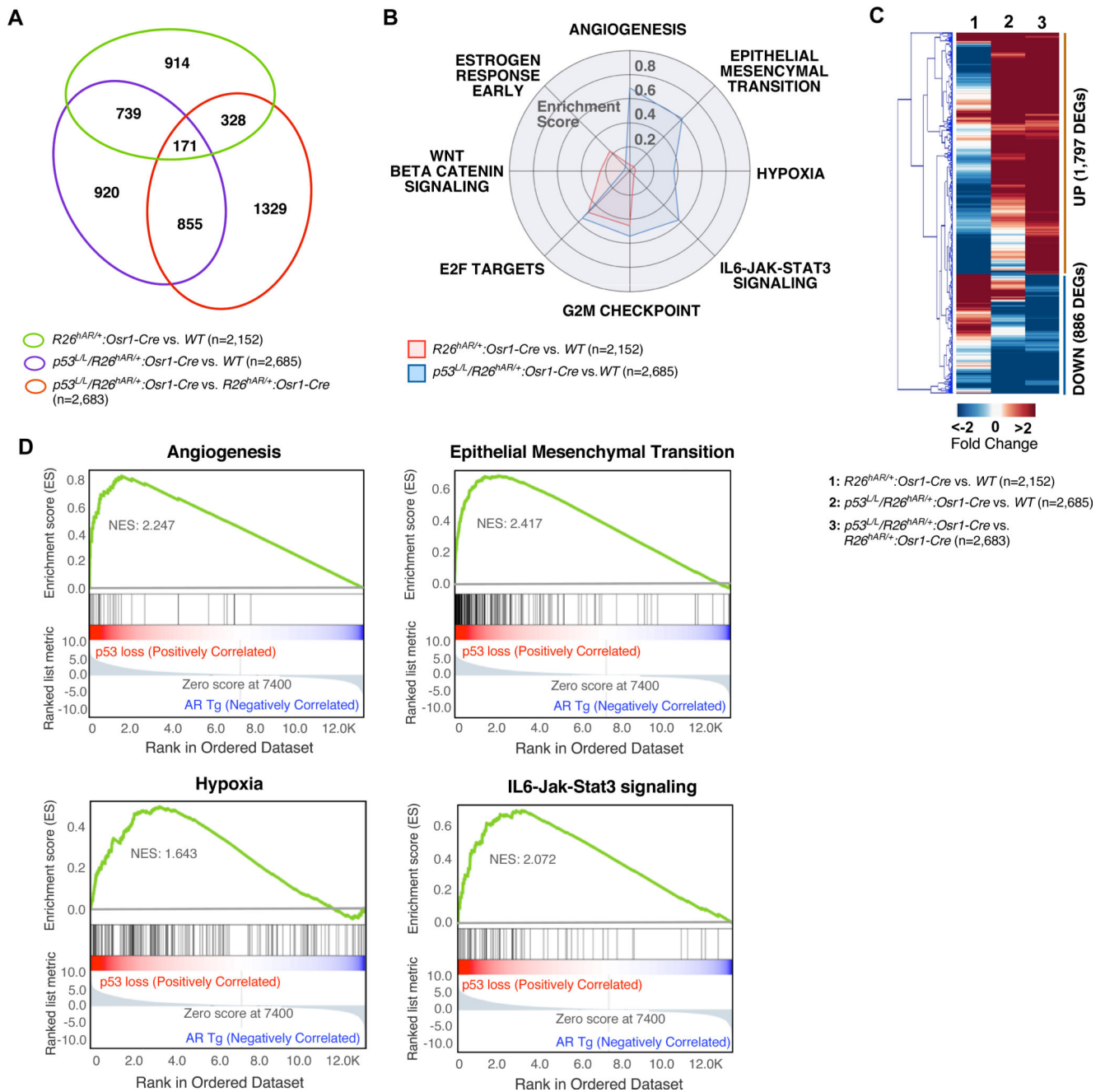
Figure 5. Enhancement of pathways associated with aggressive tumor phenotype and disease progression in prostate tumors with *AR* transgene expression and deletion of *Trp53*
A. Venn diagram of differentially expressed genes between different genotype mice as labeled above. **B**. Radar chart displays differential enrichment of *R26^{hAR/+}:Osr1-Cre* mice and *p53^{L/L}/R26^{hAR/+}:Osr1-Cre* mice in comparison with controls. Red and blue lines indicate enriched hallmark gene sets in *R26^{hAR/+}:Osr1-Cre* and *p53^{L/L}/R26^{hAR/+}:Osr1-Cre* mice, respectively. **C**. Heat map of differentially expressed genes (DEGs) from the indicated comparisons. **D**. GSEA results of hallmark gene sets significantly enriched in *p53^{L/L}/R26^{hAR/+}:Osr1-Cre* versus *R26^{hAR/+}:Osr1-Cre* mice.
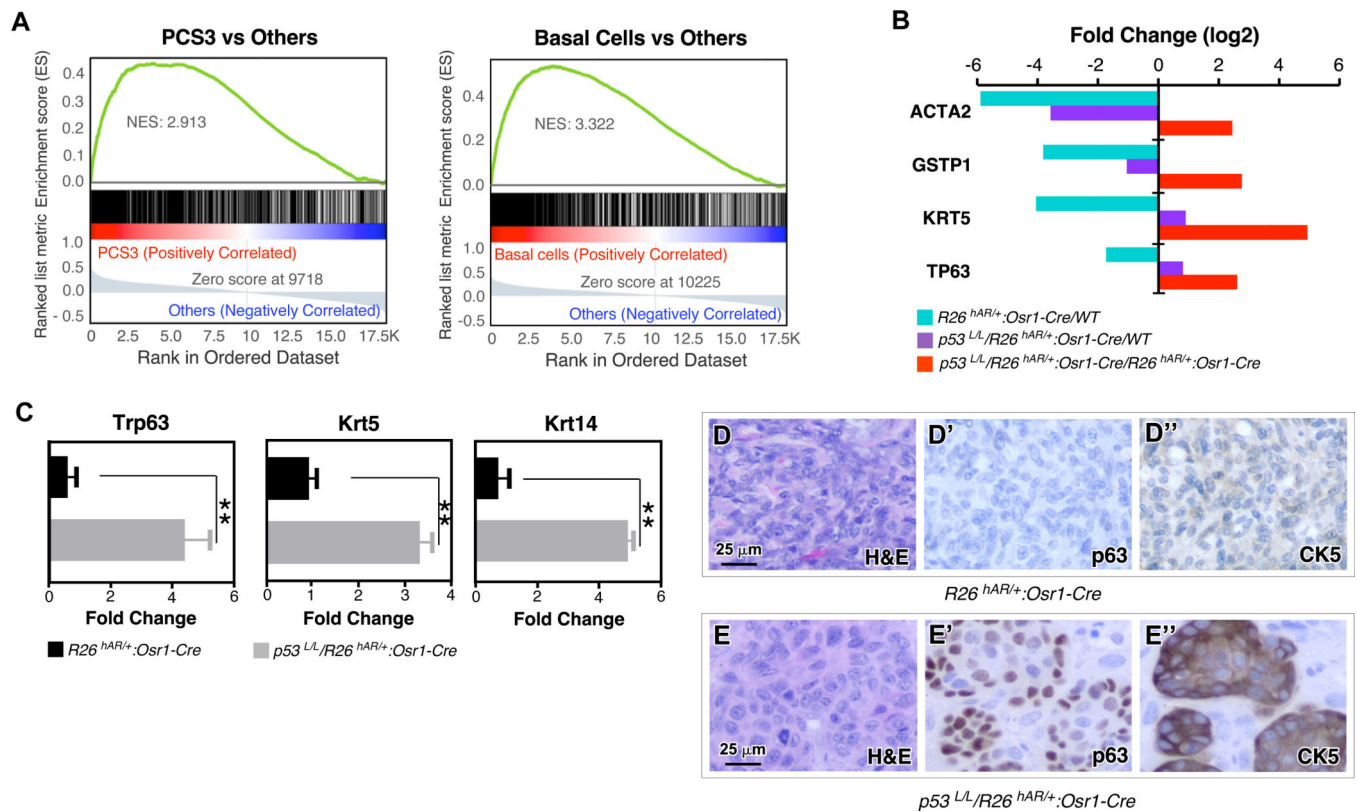
Figure 6. Transgenic *AR* expression combined with *Trp53* loss induces prostatic basaloid cell tumor development.

A. GSEA plots display significant enrichment in PCS3 and Basal subtypes of the DEGs from *p53^{L/L}/R26^{hAR/+}:Osr1-Cre* versus *R26^{hAR/+}:Osr1-Cre* mice. Genes were ranked with fold changes by comparing between PCS subtypes or between PAM50 subtypes to compute GSEA results using the Prostate Cancer Transcriptome Atlas (PCTA). **B**. Bar plot of prostate basal marker gene expression from mice of the indicated genotypes. **C**. qRT-PCR analysis of basal cell markers from mice of the indicated genotypes. Significance determined by Students' T test and data were represented as + SD (n=3 replicated per data point); ** p<0.01, ***p<0.001. **D-E**. Representative H&E or IHC of prostatic tumor lesions from *R26^{hAR/+}:Osr1-Cre* or *p53^{L/L}/R26^{hAR/+}:Osr1-Cre* mice using the indicated antibodies. Scale bar: 25 μm.
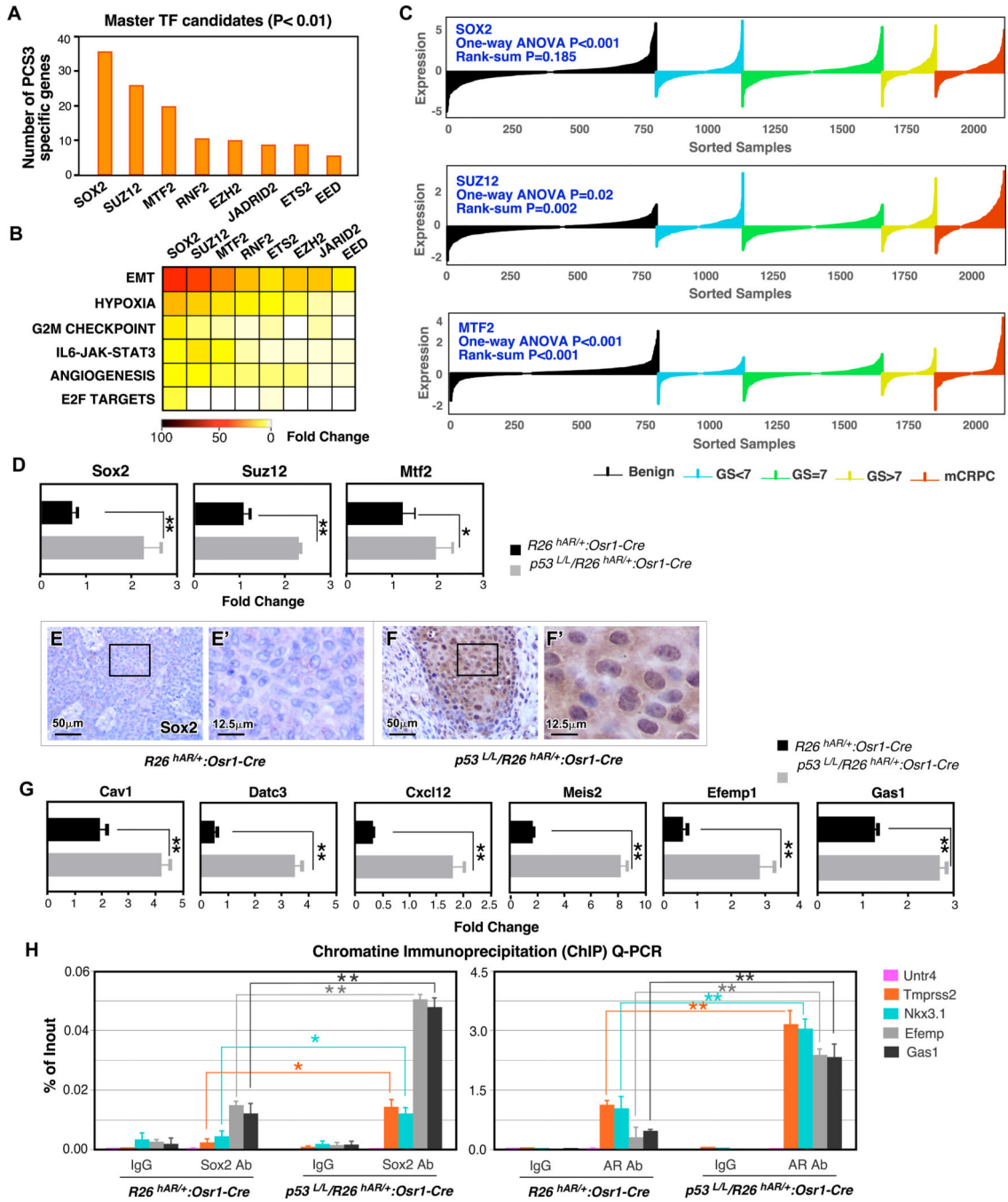
Figure 7. *SOX2* expression is increased in basal cell tumors with transgenic AR expression and loss of P53.

A. Bar plot of up-regulated genes in *p53^{L/L}/R26^{hAR/+}:Osr1-Cre* compared to *R26^{hAR/+}:Osr1-Cre*, that are involved in the genes having significantly high expression in PCS3 subtype, for each master TF candidates. **B**. Heat map of up-regulated target genes for each master TF candidate in *p53^{L/L}/R26^{hAR/+}:Osr1-Cre* compared to *R26^{hAR/+}:Osr1-Cre* involved in the indicated hallmark gene sets. EMT: epithelial to mesenchymal transition. **C**. Lollipop plots showing expression of top 3 master TFs in the Prostate Cancer Transcriptome

Atlas (PCTA). One-way ANOVA with two-tailed test across 6 different disease statuses and two-tailed Rank-Sum test for primary versus metastatic tumor samples were performed. **D**. RT-qPCR analysis of the master regulator candidates in tumor samples from the indicated mice. Significance determined by Students' T test and data were represented as + SD (n=3 replicated per data point); ** p<0.01 **E-F**. Representative IHC stains with SOX antibody in prostatic tumor samples of genotype as indicated above. Scale bar: 50 μm or 12.5 μm. **G**. qRT-PCR analysis of SOX2-regulated genes highly expressed in the PCS3 subtype in *p53$^{L/L}$/R26$^{hAR/+}$:Osr1-Cre* versus *R26$^{hAR/+}$:Osr1-Cre* mice. Significance determined by Students' T test and data were represented as ± SD (n=3 replicated per data point); ** p<0.01. **H**. SOX2 ChIP-qPCR (left panel) and AR ChIP-qPCR (right panel) of SOX2 target genes (*Efemp & Gas1*) as well as AR target genes (*Tmprss2 & Nkx3.1*), and negative control (*Untr4*) shown as percent input. Significance determined by Students' T test and data were represented as ± SD (n=3 replicated per data point); * p<0.05, ** p<0.01.